

# Rigorous $Q$ Factor Formulation and Characterization for Nonlinear Oscillators

Tianshi Wang and Jaijeet Roychowdhury

The Department of Electrical Engineering and Computer Sciences, The University of California, Berkeley, CA, USA

Email: {tianshi, jr}@berkeley.edu

**Abstract**—In this paper, we discuss the definition of  $Q$  factor for nonlinear oscillators. While available definitions of  $Q$  are often limited to linear resonators or oscillators with specific topologies, our definition is applicable to any oscillator as a figure of merit for its amplitude stability. It can be formulated rigorously and computed numerically from oscillator equations. With this definition, we calculate and analyze the  $Q$  factors of several oscillators of different types. The results confirm that the proposed  $Q$  formulation is a useful addition to the characterization techniques for oscillators.

## I. Introduction

The concept of quality factor, or  $Q$  factor, is one that is applicable in many fields of engineering. The  $Q$  factor is a dimensionless parameter that describes how “lossy” an oscillator is. A higher  $Q$  factor has many implications. It is often taken as synonymous with the stability of the oscillator in both amplitude and frequency, which then translates to better energy efficiency and lower phase noise — the “quality” is higher. However, once we try to write down an exact formula for the  $Q$  factor of an oscillator, several confusions arise.

Firstly,  $Q$  factor is often defined under the context of (usually second-order) linear resonators, which are systems with damped oscillatory behaviours. There are several definitions. One is the frequency-to-bandwidth ratio of the resonator:

$$Q \stackrel{\text{def}}{=} \frac{f_r}{\Delta f} = \frac{\omega_r}{\Delta \omega}. \quad (1)$$

The formula implies that there is a Bode plot of the system with a resonance frequency, thus is only meaningful for BIBO stable linear systems with well-defined inputs and outputs. It is not directly applicable to oscillators which are by-definition autonomous and usually nonlinear. Another definition for  $Q$  factor is from the energy perspective:

$$Q \stackrel{\text{def}}{=} \frac{\text{Energy Stored}}{\text{Energy Dissipated per Cycle}}. \quad (2)$$

This assumes that there is damping in the oscillation, which is not true for self-sustaining oscillators. There are other definitions that directly map  $Q$  to a parameter in the transfer function, but they are limited to linear systems as well.

These definitions are rigorous and clear for linear resonators, and they are widely-used in the design of integrated inductors and tuned band-pass filters. But they are not directly applicable to, and are often misused in the characterization of nonlinear oscillators. This leads to another common confusion — people often simply assume an oscillator to have the same  $Q$  factor as the resonator it is using inside. For example, an LC oscillator is often said to have the same  $Q$  as the linear RLC circuit in it. However, this is not true. An obvious counterexample is that the use of a high- $Q$  resonator inside does not guarantee a high- $Q$  oscillator; one has to be careful in the design of the nonlinear circuit around it in order not to introduce too much distortion or power loss.

For oscillators, one may extend the  $Q$  definition in (2) to undamped oscillation. This requires manually identifying energy storage components and integrating energy dissipations. It depends heavily on the topology of the oscillator and is only applicable to several types of LC oscillators. Another approach attempts to extend the frequency-domain characterization technique in (3) to feedback oscillators. The oscillator is assumed to have a feedback block-diagram model with an open-loop transfer function. This implies linearization of the nonlinear components at the amplitude of oscillation, analogous to the describing function analysis. The transfer function is then assumed to have a resonance frequency, where the slope of its phase with respect to frequency gives an “open-loop  $Q$ ” [1]. The higher the open-loop  $Q$ , the sharper the phase slope, and the more resistant the closed-loop system to the variations in the frequency of oscillation. Similar open-loop  $Q$  concept can also be defined using S-parameter transfer functions [2]. More recently, the relationship between this  $Q$  definition and the phase noise performances are discussed for oscillators with one- and two-port passive linear networks [3]. These  $Q$  definitions offer useful insights into an oscillator’s frequency stability. But for these frequency-domain, transfer-function-based techniques to be applicable, specific circuit topology, sinusoidal waveforms and the presence of a resonant subcircuit have to be assumed.

Another widely-used definition of  $Q$  factor in oscillator measurements is arguably adapted from (3). It also uses a frequency-to-linewidth ratio:

$$Q \stackrel{\text{def}}{=} \frac{f}{\Delta f_{3dB}}, \quad (3)$$

where  $f_{3dB}$  is the 3dB linewidth of the spectrum of the oscillator’s output. This  $Q$  factor can be conveniently measured using a spectrum analyzers, but it is arguable if this quality factor is a property intrinsic to the oscillator. The linewidth depends on the noise sources in the circuit — their types, magnitudes, and locations. This indicates that  $Q$  factor defined in this way will be affected by temperature and interferences. And numerical calculation of this  $Q$  factor won’t be feasible without knowing the noise model associated with the oscillator; the characterization cannot be performed from just oscillator equations.

In this paper, we discuss a new definition of  $Q$  factor that can be applied to any oscillator. It can be conveniently measured, rigorously formulated and numerically computed. It is defined from the energy perspective, in close analogy to the linear resonator case in (2). Instead of analyzing the total energy storage, we add (or subtract) a small amount of extra energy to the oscillator by perturbation. The oscillator will settle back to its amplitude-stable state eventually, dissipating (or restoring) a fraction of the extra energy every cycle. The speed in which the oscillator settles back indicates how amplitude-stable it is, reflecting the energy efficiency of the oscillator; we can then

define  $Q$  factor based on it. We expand on this idea in Sec. II. As it turns out, there is a better way to formulize and characterize this  $Q$  factor than directly applying perturbation and observing amplitude decay. The energy-based intuition in Sec. II leads to a more mathematically rigorous and general formulation of the proposed  $Q$  factor, which is closely related to Floquet theory, and can be calculated numerically from oscillator equations. We discuss the formulation and numerical characterization in more detail in Sec. III and Sec. IV respectively. We then try the numerical techniques on several oscillators of different types, including ring oscillators, LC oscillators, spin torque oscillators, and a chemical reaction oscillator in Sec. V. The examples confirm that the proposed  $Q$  factor formulation matches the intuition behind quality factor and offers a good measure of an oscillator's amplitude settling behaviour.

In Sec. V, we also discuss the differences and relationship between our new  $Q$  factor definition and the other energy-based one in (2) in the context of LC oscillators. We emphasize that the proposed  $Q$  factor formulation is indeed different and more suitable for characterizing amplitude stability. In Sec. VI, we further summarize and compare definitions of  $Q$  for both linear resonators and nonlinear oscillators. While the frequency- and energy-based definitions of  $Q$  for second-order linear resonators are equivalent, different  $Q$  definitions for oscillators are not. The  $Q$  formulation we propose is a useful addition to the figures of merit of oscillators, especially in applications that require fast amplitude settling, *e.g.*, low distortion, amplitude-enhanced VCOs [4, 5], oscillator-based computation systems [6, 7], *etc.*

## II. Intuition Behind the New $Q$ Definition

Figure 1 compares the waveforms of two oscillators. Even without any definition, it is easy to tell that the LC oscillator should have a higher  $Q$ , since its settling behaviour is much slower, indicating more stability in amplitude. The definition of  $Q$  should match this intuition.

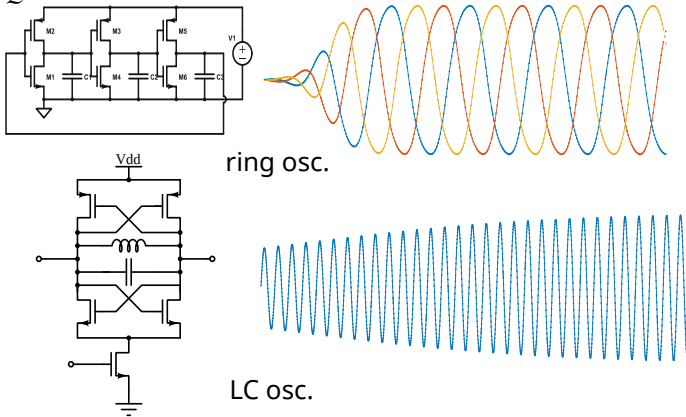


Fig. 1: Intuition behind  $Q$  factor: LC oscillator (high- $Q$ ) settles more slowly in amplitude than ring oscillator (low- $Q$ ).

We define  $Q$  from the energy perspective, similar to (2). Consider perturbing an oscillator with a small amount of extra energy; the oscillator settles back to its stable orbit gradually. We can then define the ratio between the extra energy applied and the energy dissipated (or restored) every cycle as the  $Q$  factor of the oscillator:

$$Q \stackrel{\text{def}}{=} \frac{\text{Extra Energy Applied}}{\text{Extra Energy Dissipated per Cycle}}. \quad (4)$$

The definition is illustrated in Figure 2 with both the time-domain waveforms and phase plane plots. It can be conveniently

measured from either transient simulations or experiments, without analyzing circuit topology or open-loop block diagrams. The higher the  $Q$  factor, the more slowly its amplitude responds to perturbations, and the more stable the amplitude of the limit cycle. These observations fit intuition.

As also illustrated in Figure 2, the  $Q$  definition for oscillators is analogous to that for the linear resonators. And the widely-used energy-based  $Q$  formulation in (2) for linear systems is in fact just a special case of our definition in (4), with the amplitude-stable state being the zero state.

Note that the definition in (4) has several limitations when applied in practice. As the oscillator is nonlinear, different amount of the extra energy introduced will have different results. Ideally, to study the properties of the limit cycle, we would like the extra energy to be as small as possible, which then makes measurement difficult when there is noise or numerical error. Also, the direction of the perturbation in the state space also affects the settling speed. Despite the limitations, the energy-based definition serves as the physical intuition behind the more rigorous definition we discuss in Sec. III.

## III. Formulation of $Q$ from LPTV Theory

To study an oscillator's response under a small perturbation, we first model the oscillator mathematically as a set of Differential Algebraic Equations (DAEs) in the following form.

$$\frac{d}{dt} \vec{q}(\vec{x}(t)) + \vec{f}(\vec{x}(t)) = \vec{0}, \quad (5)$$

where  $\vec{x}(t) \in \mathbb{R}^n$  contains the time-varying unknowns, or states in the oscillator system;  $\vec{q}$  and  $\vec{f}$  are vector functions with the same size as  $\vec{x}(t)$ .

The oscillator system is autonomous, *i.e.*, DAE (5) has no time-varying inputs, but the steady state response is time-varying and periodic, *i.e.*, there exists a non-constant response  $\vec{x}_s(t)$  satisfying (5) and a time period  $T > 0$ , such that

$$\vec{x}_s(t) = \vec{x}_s(t + T). \quad (6)$$

If the oscillator starts at  $t = 0$  with  $\vec{x}_s(0)$ ,  $\vec{x}_s(t)$  will be its response. Now we consider perturbing the initial condition by a small  $\Delta\vec{x}_0$ , the response for  $t \geq 0$  will satisfy

$$\frac{d}{dt} \vec{q}(\vec{x}_s(t) + \Delta\vec{x}(t)) + \vec{f}(\vec{x}_s(t) + \Delta\vec{x}(t)) = \vec{0}, \quad (7)$$

with

$$\Delta\vec{x}(0) = \Delta\vec{x}_0, \quad (8)$$

where the time-varying vector  $\Delta\vec{x}(t)$  captures the derivation of the oscillator's response under perturbation from its steady state  $\vec{x}_s(t)$ .

If  $\Delta\vec{x}(t)$  is always small with its magnitude decaying over time, the trajectory  $\vec{x}_s(t) + \Delta\vec{x}(t)$  is close to  $\vec{x}_s(t)$ . Linearizing  $\vec{q}$  and  $\vec{f}$  along  $\vec{x}_s(t)$  results in a Linear Periodic Time Varying (LPTV) system as in (9), which gives a good approximation to the original system in (7).

$$\frac{d}{dt} \mathbf{C}(t) \cdot \Delta\vec{x}(t) + \mathbf{G}(t) \cdot \Delta\vec{x}(t) = \vec{0}, \quad (9)$$

where  $\mathbf{C}(t)$  and  $\mathbf{G}(t)$  are time-varying,  $T$ -periodic matrices.

$$\mathbf{C}(t) = \left. \frac{d\vec{q}}{d\vec{x}} \right|_{\vec{x}_s(t)}, \quad \mathbf{G}(t) = \left. \frac{d\vec{f}}{d\vec{x}} \right|_{\vec{x}_s(t)}. \quad (10)$$

As it turns out, the assumption that  $\Delta\vec{x}(t)$  decays with time is not always true for arbitrary perturbations; there are constraints on  $\Delta\vec{x}_0$  for the approximation to hold. We will concretize these constraints as we proceed with our discussion.

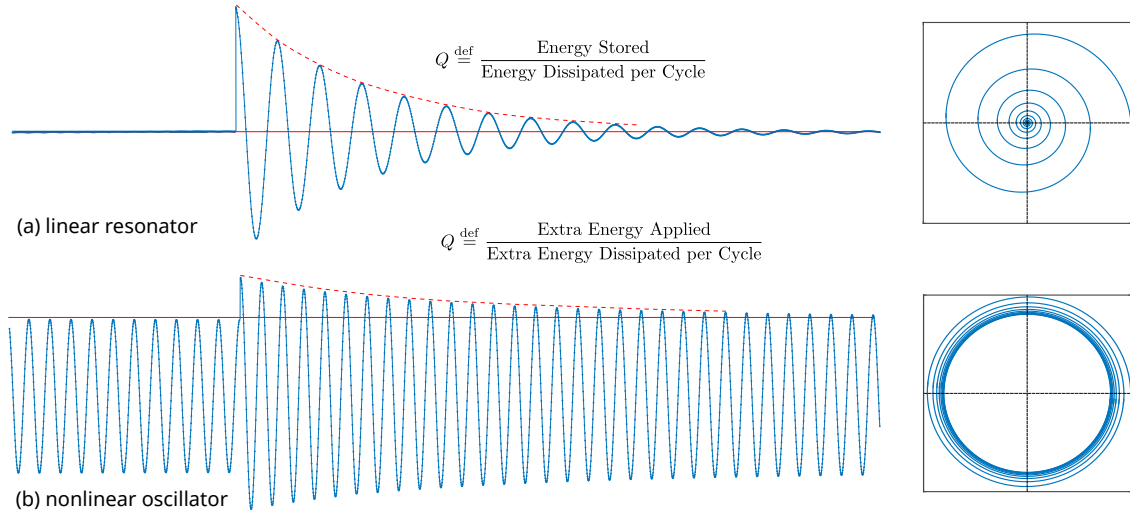


Fig. 2: Illustration of the definition of  $Q$  factor for nonlinear oscillators.

In order to analyze the LPTV system in (9), we consider solving for the fundamental matrix associated with it. The fundamental matrix of a LPTV system is the time-varying matrix solution  $\mathbf{X}(t) \in \mathbb{R}^{n \times n}$  to the following matrix DAE.

$$\frac{d}{dt} \mathbf{C}(t) \cdot \mathbf{X}(t) + \mathbf{G}(t) \cdot \mathbf{X}(t) = \vec{0}, \quad (11)$$

with

$$\mathbf{X}(0) = \mathbf{I}_n. \quad (12)$$

$\mathbf{X}(t)$  at a given time  $t$  can be calculated numerically through time-integration. Once  $\mathbf{X}(t)$  is calculated, for any small initial perturbation  $\Delta \vec{x}_0$ ,  $\Delta \vec{x}(t)$  is simply given as

$$\Delta \vec{x}(t) = \mathbf{X}(t) \cdot \Delta \vec{x}_0, \quad t \geq 0. \quad (13)$$

In particular,  $\Delta \vec{x}(T) = \mathbf{X}(T) \cdot \Delta \vec{x}_0$  captures the changes to the initial perturbation  $\Delta \vec{x}_0$  after one cycle of oscillation. According to Floquet theory [8], there exists a time-invariant matrix  $\mathbf{F}$  such that

$$\mathbf{X}(t) = \mathbf{U}(t) \cdot e^{\mathbf{F}t} \cdot \mathbf{V}^*(t), \quad (14)$$

where  $\mathbf{U}(t)$  and  $\mathbf{V}(t)$  are  $T$ -periodic, non-singular matrices.

The eigenvalues of matrix  $\mathbf{F}$ , namely  $\{\mu_k\}$ , are known as the *Floquet exponents*. The eigenvalues of matrix  $\mathbf{X}(T)$ , namely  $\{\lambda_k\}$ , can then be expressed as

$$\lambda_k = e^{\mu_k T}. \quad (15)$$

$\{\lambda_k\}$  are known as *characteristic multipliers*. Their moduli  $\{|\lambda_k|\}$  can be calculated from the real parts of  $\{\mu_k\}$ , which are also called *Lyapunov exponents* [8]. This  $\{\lambda_k\}$  spectrum of matrix  $\mathbf{X}(T)$  gives us comprehensive information on the changes of  $\Delta \vec{x}_0$  after one cycle of oscillation.

It is provable that the oscillation is self-sustaining if and only if there exists a *characteristic multiplier* exactly equal to 1 [9]. This means that part of the initial perturbation  $\Delta x_0$  will never disappear; it represents the phase change of the oscillation after perturbation. Without loss of generality, we assume  $\lambda_1 = 1$ , and then arrange the rest of  $\{\lambda_k\}$  in descending order of their moduli. Among them, the one with the largest modulus is  $\lambda_2$ . If  $|\lambda_k| < 1$  for  $k \geq 2$ , and  $\Delta x_0$  doesn't contain any component aligned with the eigenvector corresponding to  $\lambda_1$ , the initial perturbation will decay with time. And the speed of decay is characterized by its slowest moment, which decreases to  $|\lambda_2|$  of its size after each cycle. If we assume that after  $Q$  cycles the size is no larger than

5% of its initial value, then

$$|\lambda_2|^Q \leq 0.05 \implies Q \geq \log_{|\lambda_2|} 0.05. \quad (16)$$

$Q$  factor can then be estimated as the value of  $\log_{|\lambda_2|} 0.05$ , or the integer closest to it.

Note that for capturing the amplitude settling behaviour precisely, we will need the whole spectrum of matrix  $\mathbf{X}(T)$ , *i.e.*,  $\{\lambda_k\}$ . The response of a LPTV system, just like that of a LTI system, consists of the superposition of components associated with all *multipliers*. However, if we were to derive a single scalar figure of merit to represent this complex settling behaviour, it is not unreasonable to consider only the slowest moment, characterized by  $\lambda_2$ .

The formulation of  $Q$  is based on the exponential decay of  $\Delta \vec{x}(t)$  after time  $T$ . We argue that it is indeed based on the definition of (4). The energy associated with a DAE is often formulated as

$$E(\vec{x}) \propto \vec{x}^T \mathbf{H} \vec{x}, \quad (17)$$

where  $\mathbf{H}$  is a symmetric matrix commonly known as the Hamiltonian of the system. Its exact formula varies from system to system. From (17), we have

$$\Delta E(\Delta \vec{x}, \vec{x}) = E(\vec{x} + \Delta \vec{x}) - E(\vec{x}) \propto \vec{x}^T \mathbf{H} \cdot \Delta \vec{x}, \quad (18)$$

where  $\mathbf{H}$  is a fixed matrix,  $\vec{x}$  is the trajectory of oscillation — both are independent of  $\Delta \vec{x}$ . Therefore, the energy decay  $\Delta E$  is equivalent to the settling of perturbation  $\Delta x$ , characterized by the same set of *characteristic multipliers*.

#### IV. Numerical Characterization

From Sec. III, the  $Q$  formulation in (16) can be computed numerically. The procedures are summarized as follows:

- 1) Compute the large-signal periodic steady state solution  $\vec{x}_s(t)$  numerically, often through the shooting method [10], or Harmonic Balance [11].
- 2) Linearize functions  $\vec{q}(\vec{x})$  and  $\vec{f}(\vec{x})$  along  $\vec{x}_s(t)$ , calculate time-varying Jacobian matrices  $\mathbf{C}(t)$  and  $\mathbf{G}(t)$ ,  $0 \leq t \leq T$ , store them as tabulated data <sup>1</sup>.
- 3) Solve for  $\mathbf{X}(T)$  through numerical time-integration of the matrix DAE (11) from its initial condition (12).
- 4) Perform eigenanalysis on  $\mathbf{X}(T)$  to obtain  $\lambda_2$ ; calculate  $Q$

<sup>1</sup> $\mathbf{C}(t)$  and  $\mathbf{G}(t)$  can be pre-computed and are often stored at the same time as the periodic steady state calculation.

factor with (16).

We note that there are well-developed numerical techniques for each step in the calculation of  $Q$ . Many implementations are already available today in open-source and commercial simulators for oscillator phase noise analysis. We point out that these implementations can be easily adapted to the analysis of amplitude stability of oscillators.

We also note that, for improved efficiency, full eigenanalysis on  $\mathbf{X}(T)$  is not necessary. Since the calculation of  $Q$  only requires  $\lambda_2$  and we know that  $\lambda_1 = 1$ , power method can be easily modified to compute only  $\lambda_2$ .

Our implementation is based on MAPP: the Berkeley Model and Algorithm Prototyping Platform [12, 13]. We plan to release it as open-source software under the GNU General Public License.

## V. Examples

After explaining the intuition, formulation and calculation of the proposed new  $Q$  definition in the previous sections, in this section, we compute and analyze the  $Q$  factors of several oscillators of different types.

### A. Ring Oscillators

#### 1) Analytical Results from Ideal Ring Oscillator

The simplest ideal ring oscillator has 3 stages, each of which consists of a memoryless ideal inverter followed by an RC delay circuit. It can be modelled using the input voltages ( $v_1, v_2$  and  $v_3$ ) of the three stages:

$$\dot{v}_1 = \frac{f(v_3) - v_1}{\tau}, \quad \dot{v}_2 = \frac{f(v_1) - v_2}{\tau}, \quad \dot{v}_3 = \frac{f(v_2) - v_3}{\tau}, \quad (19)$$

where  $\tau$  is the time constant of the RC circuit at each stage;  $f(v)$  represents the I/O relationship of the ideal inverter:

$$f(v) = \begin{cases} -1, & \text{if } v \geq 0, \\ +1, & \text{otherwise.} \end{cases} \quad (20)$$

The reason for considering this ideal ring oscillator is that, despite its simplicity, it is well suited for estimating both qualitative and quantitative features of ring oscillators [14], and its fundamental matrix solution is available analytically [14].

The three eigenvalues of  $\mathbf{X}(T)$  are  $\lambda_1 = 1$ ,  $\lambda_2 = \phi^{-6}$ ,  $\lambda_3 = \phi^{-12}$ , where  $\phi = (\sqrt{5} + 1)/2 \approx 1.618$  is known as the golden ratio.

In this case,  $\lambda_2 = \phi^{-6} \approx 0.0557$ . Therefore,  $Q \approx 1.1$ . This matches intuition, as the ideal ring oscillator dissipates all of its energy after every cycle of oscillation, thus restoring to its stable amplitude very quickly.

#### 2) Numerical Results from CMOS Ring Oscillator

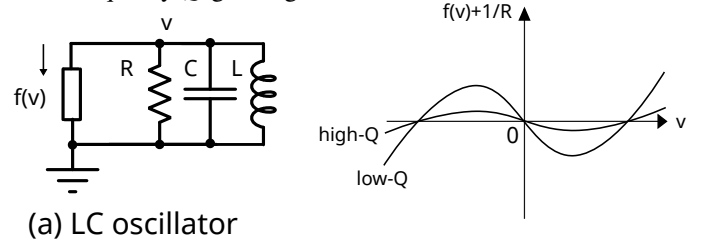
To test the numerical characterization techniques in Sec. IV, we simulate a more realistic 3-stage CMOS ring oscillator with BSIMv3.3 models. The circuit schematic is the same as in Figure 1; the waveform is also similar to the one in it. As we can see, the waveform looks almost sinusoidal, without the sharp turns in the ideal ring oscillator case. But numerical computation reveals that  $\lambda_2 \approx 0.067$ .  $Q$  is still close to 1, even though the waveform is less distorted. The oscillator's amplitude stability information is indeed embedded in its equations. And our  $Q$  formulation captures it truthfully.

### B. LC Oscillators

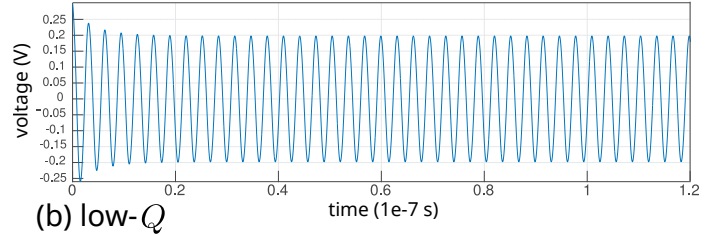
#### 1) High- $Q$ and Low- $Q$ Negative Resistance LC Oscillators

Here we consider a simple negative-resistance LC oscillator circuit shown in Figure 3. Different nonlinearities in  $f(v)$  result

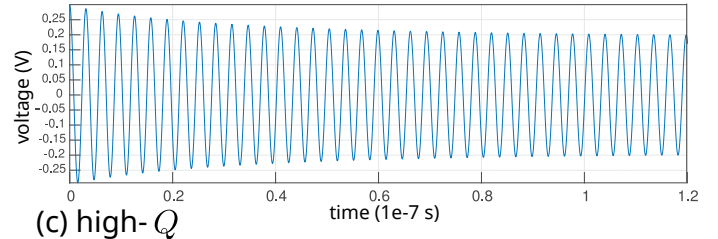
in different  $Q$  factors. Intuitively, as  $f(v) + \frac{1}{R}$  gets “flatter”, the oscillator will appear more like an LC tank with no resistance, thus the quality  $Q$  gets higher.



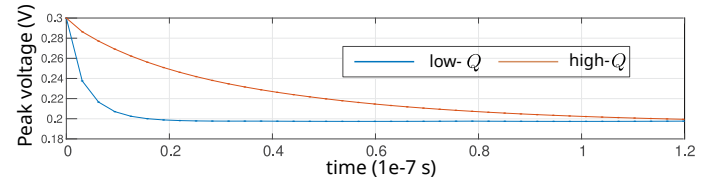
(a) LC oscillator



(b) low- $Q$



(c) high- $Q$



(d) amplitude difference

**Fig. 3:** (a) A simple negative-resistance LC oscillator. Different choice of  $f(v)$  will result in different  $Q$  factor of the oscillator. (b-d) the changes of amplitudes after perturbations for low- $Q$  and high- $Q$  LC oscillators.

We choose  $L = 0.5nH$ ,  $C = 0.5nF$ ,  $f(v) = K \cdot (v - \tanh(1.01 \cdot v))$  for the LC oscillator. We choose  $K$  values as 1 and 20, the former results in a high- $Q$  oscillator, the latter low- $Q$ . Numerical  $Q$  factor characterization results in  $\lambda_2 \approx 0.54$  for the former, and  $\lambda_2 \approx 0.94$  for the latter, indicating  $Q$  factors of 4.8 and 48 respectively.

The transient simulation results in Figure 3 confirm that the high- $Q$  one indeed settles much more slowly in amplitude.

#### 2) $Q$ Factor and Energy Dissipation

In the circuit in Figure 3, the inductor and capacitor are ideal devices that do not dissipate any energy. When the circuit exhibits self-sustaining oscillation, the energy dissipated by the resistor and that generated by the negative resistance component should balance out in every cycle. If we assume the voltage waveform at the only non-ground node in the circuit to be sinusoidal as  $v(t) = V_{\max} \sin(\omega t)$ , the two energies per cycle can be plotted as in Figure 4.

In Figure 4 we have chosen a slightly different set of parameters with  $f(v) = K \cdot (v - \tanh(2 \cdot v))$  such that the curves are more clearly separated. From Figure 4, we observe that between

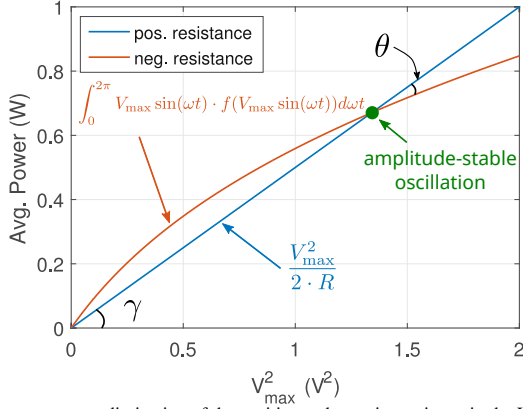


Fig. 4: Average power dissipation of the positive and negative resistors in the LC oscillator in Figure 3. Their intersection indicates self-sustaining oscillation. The angle  $\theta$  characterizes how amplitude-stable the oscillation is.

$V_{\max} = 0$  and the oscillation point, the negative resistance device generates more energy per cycle than that dissipated by the positive resistor. Therefore, the oscillation cannot be stable and the amplitude will build up. On the other hand, when  $V_{\max}$  is beyond the oscillation point, the amplitude of oscillation will decrease. Therefore, only at the oscillation point will the two energies balance out and the amplitude be stable. The angle  $\theta$  then characterizes how fast amplitude settles back to this equilibrium. More specifically, if  $V_{\max}^2$  changes by  $\delta$ ,  $(\tan(\gamma + \theta) - \tan(\gamma)) \cdot \delta$  captures how much extra energy will be dissipated or restored in one cycle of oscillation. This is to say,  $1 - (\tan(\gamma + \theta) - \tan(\gamma))$  is proportional to  $|\lambda_2|$ . Given  $\gamma$ , the larger the value of  $\theta$ , the smaller the value of  $|\lambda_2|$ , and the lower the  $Q$  factor. This offers a graphical interpretation of the  $Q$  factor for this particular type of LC oscillator.

In comparison, we consider the  $Q$  definition in (2). In this LC circuit, the definition is applicable since we can identify the energy storage and dissipation components. At the oscillation point, the two average powers in Figure 4 are equal. Therefore, the angle  $\gamma$ , determined only by the positive resistor, will characterize the energy dissipation in the  $Q$  definition. This  $Q$  definition doesn't use any information from the nonlinearity in the circuit, nor does it provide any information related to the oscillation point, *e.g.*, the angle  $\theta$ . It captures the energy dissipation correctly, but it doesn't characterize the amplitude stability of the oscillator.

In conclusion, these two definitions correspond to different properties in the energy plot; they characterize different attributes of the oscillator.

### C. BJT Phase-shift Oscillator

The  $Q$  factors of ring oscillators and LC oscillators are straightforward to understand; our calculations match the intuitions behind them. But unlike conventional  $Q$  definitions, our formulation works for general nonlinear oscillators beyond these two well-studied types.

A typical BJT phase-shift oscillator as shown in Figure 5 consists of an inverting BJT amplifier and a phase-shift RC network that feeds the delayed output as the input to the amplifier. It does not require an inductor to oscillate, and there is no band-pass linear resonator in the oscillator; defining the  $Q$  factor by identifying energy storage devices becomes less relevant. But our  $Q$  formulation can still be applied.  $\lambda_2$  for the circuit in Figure 5 is 0.9081, corresponding to a  $Q$  factor of 31. The results show that although there is no inductor, the oscillator does not behave like a ring oscillator, which settles to

the limit cycle very fast. Instead, the oscillation builds up after several cycles. This observation for the  $Q$  factor characterization can be confirmed with transient simulations as well, *e.g.*, in Figure 6. In this case, for transient simulation to show the amplitude settling behaviour, initial guesses that are far away enough from the limit cycle have to be used. And as the system has multiple dimensions, randomly chosen initial guesses will show different amplitude settling speed; they won't capture the worst case that defines the  $Q$  factor. In comparison, the LPTV-based characterization is more rigorous and more accurate in measuring the stability of the limit cycle.

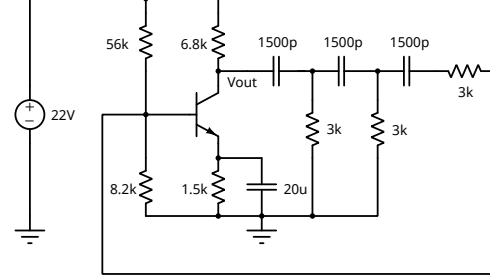


Fig. 5: Schematic of a BJT phase-shift oscillator.

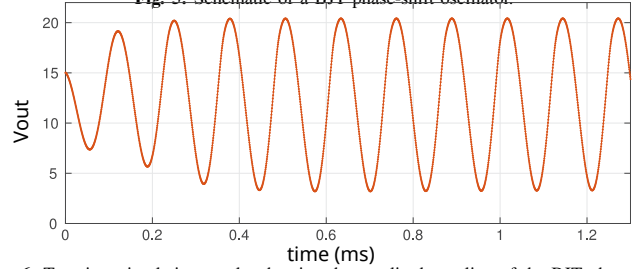


Fig. 6: Transient simulation results showing the amplitude settling of the BJT phase-shift oscillator.

### D. Spin Torque Nano-Oscillator (STNO): LLG Equation

Magnetization in a STNO, often represented with a 3D vector  $\mathbf{M}$ , can vary internally in response to torques  $\mathbf{H}_{\text{ext}}$ . The rotation of  $\mathbf{M}$  is predicted by the Landau-Lifshitz-Gilbert (LLG) equation (adapted and simplified from [15]):

$$\tau \frac{d\mathbf{M}}{dt} = -\mathbf{M} \times \mathbf{H}_{\text{eff}} - \alpha \mathbf{M} \times (\mathbf{M} \times \mathbf{H}_{\text{eff}}) - \alpha \mathbf{M} \times (\mathbf{M} \times \mathbf{I}_s), \quad (21)$$

where

$$\mathbf{H}_{\text{eff}} = \mathbf{H}_{\text{int}} + \mathbf{H}_{\text{ext}} = [K_x, K_y, K_z]^T \cdot \mathbf{M} + \mathbf{H}_{\text{ext}}. \quad (22)$$

Parameter Name	Value
$\tau$	1e-9
$\alpha$	0.02
$K_x$	-10
$K_y$	0
$K_z$	1
$\mathbf{I}_s$	$[0, 0, -0.6\text{mA}]^T$
$\mathbf{H}_{\text{ext}}$	$[0, 0, 2]^T$

TABLE I: Parameters and inputs for the LLG equation of a STNO.

Both inputs  $\mathbf{H}_{\text{ext}}$  and  $\mathbf{I}_s$  are 3D vectors. When they have appropriate values, the magnetization vector  $\mathbf{M}$  can begin self-sustaining oscillation, which generates an oscillating voltage across the device. An example set of parameters that can generate oscillating  $\mathbf{M}$  is given in Table I.

There are no inductors or capacitors in the system; identifying energy storage is not straightforward. It is not clear what the

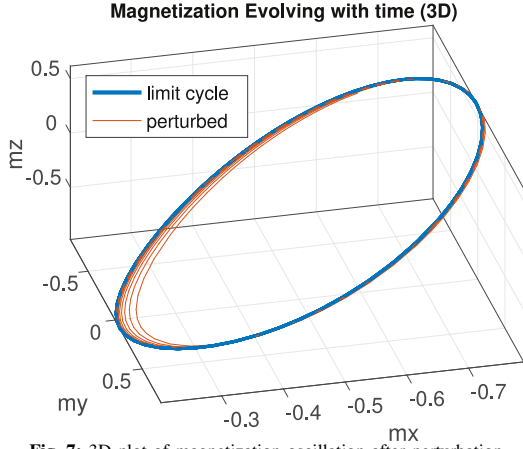


Fig. 7: 3D plot of magnetization oscillation after perturbation.

noise sources are in the system.<sup>2</sup> The only way for characterizing  $Q$  is by fabricating the oscillator and measuring it with a spectrum analyzer; conventional  $Q$  characterizations cannot be carried out with system equations in (21) and (22). In comparison, our formulation of  $Q$  still applies. With the set of parameter listed in Table I, we simulate a STNO and show results in Figure 7.  $Q$  characterization shows that  $\lambda_2 \approx 0.9712$ ,  $Q \approx 103$ . We note that the slow amplitude settling behaviour is due to the nonlinear resonator inside the oscillator, which is passive and under-damped just like an RLC tank. Because of the nonlinearity, conventional Bode-based analysis cannot be performed. But the limit cycle is relatively stable compared with ring oscillators; it behaves more like LC oscillator. Our  $Q$  characterization matches this intuition. These results show the generality of our approach — the  $Q$  formulation is not limited to oscillators with linear resonators; it is not limited to electrical oscillators either.

### E. A Chemical Reaction Oscillator

Here we consider a set of chemical reactions that constitute a chemical oscillator.



The oscillator is nonlinear, with the concentrations of the three species as its states. In this case, it is not clear how to identify the energy loss in the system, or to make any analogy to commonly-known electrical oscillators; conventional  $Q$  factor definitions and characterization techniques are not applicable. In comparison, our  $Q$  factor formulation still works and can capture interesting properties of this oscillator.

Numerical calculation of  $\lambda_2$  returns an almost perfect 1, up to 14 digits, indicating an almost infinite  $Q$  factor. Put in other words, the fundamental matrix  $\mathbf{X}(T)$  has two eigenvalues equal to 1, indicating that both the phase and amplitude of this oscillator are unstable. This indeed matches intuition. Starting from different random initial concentrations of the three species, oscillations can be observed to happen on planes governed by the conservation law of this chemical system. A perturbation to the states can knock the limit cycle to a nearby plane, and the extra energy is never dissipated. These can be confirmed with

<sup>2</sup>It is often assumed that noise is another  $\mathbf{H}_{\text{noise}}$  magnetic field term added to (21). But study showing good match of this modelling assumption and measurements is still lacking.

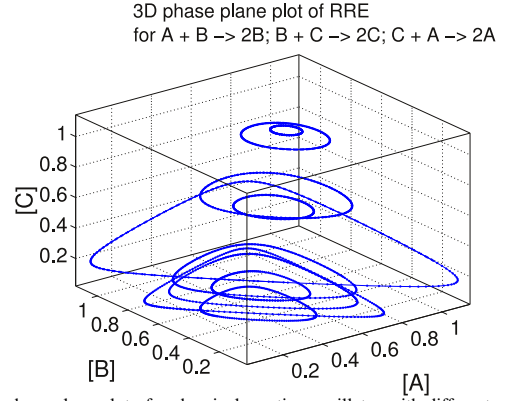


Fig. 8: 3D phase plane plot of a chemical reaction oscillator with different random initial concentrations.

transient simulation results in Figure 8.

## VI. Comparison of Different $Q$ factor Definitions

For second-order linear resonators,  $Q$  factor is well defined, with two definitions — one based on the frequency-domain representation, the other from the energy perspective. We have introduced them in Sec. I. Here we formulate them again, with names  $Q_{I1}$  and  $Q_{I2}$ .

The frequency-domain definition  $Q_{I1}$  is based on the Bode plot of the system:

$$Q_{I1} \stackrel{\text{def}}{=} \frac{f_r}{\Delta f} = \frac{\omega_r}{\Delta\omega}, \quad (26)$$

where  $\Delta f$  is the 3dB bandwidth of the Bode plot.

The energy-based definition  $Q_{I2}$  is

$$Q_{I2} \stackrel{\text{def}}{=} \frac{\text{Energy Stored}}{\text{Energy Dissipated per Cycle}}. \quad (27)$$

For second-order linear systems, these two definitions are equivalent and are often used interchangeably. To see this, we consider the transfer function of a second-order resonator:

$$H(s) = \frac{Y(s)}{X(s)} = \frac{2\zeta\omega_0 \cdot s}{s^2 + 2\zeta\omega_0 \cdot s + \omega_0^2}, \quad (28)$$

where  $X(s)$  and  $Y(s)$  are the Laplace transform of the input and output respectively. When input  $x(t)$  is an impulse, the output is

$$y(t) = A \cdot e^{-\zeta\omega_0 t} \cdot \cos(\omega_0 \cdot \sqrt{1-\zeta^2} \cdot t + \phi), \quad (29)$$

where  $A$  and  $\phi$  depend on the initial condition of the system and the size of the impulse. The resonance frequency is  $\omega_r = \omega_0 \cdot \sqrt{1-\zeta^2}$  rad/s, or  $f_r = \frac{\omega_0 \cdot \sqrt{1-\zeta^2}}{2\pi}$  Hz.

The magnitude of the Bode plot is

$$|H(j\omega)| = \frac{2\zeta\omega_0\omega}{|\omega_0^2 - \omega^2 + j2\zeta\omega_0\omega|}. \quad (30)$$

At the peak of the Bode plot,  $s = j\omega_r$ . When the system is under-damped,  $\zeta$  is small,  $\omega_r \approx \omega_0$ . Therefore,

$$|H(j\omega_r)| \approx 1. \quad (31)$$

The 3dB bandwidth corresponds to two frequencies  $\omega_{1,2}$  where  $|H(j\omega_{1,2})| \approx 1/\sqrt{2}$ . This indicates

$$|\omega_0^2 - \omega_{1,2}^2| = |2\zeta\omega_0\omega_{1,2}|, \quad (32)$$

which results in

$$\omega_{1,2} = \omega_0 \cdot (\sqrt{\zeta^2 + 1} \pm \zeta). \quad (33)$$

The 3dB bandwidth is

$$\Delta\omega = \omega_2 - \omega_1 = 2\zeta\omega_0. \quad (34)$$

$Q_{l1}$  can then be written as

$$Q_{l1} \stackrel{\text{def}}{=} \frac{\omega_r}{\Delta\omega} = \frac{\omega_0 \cdot \sqrt{1-\zeta^2}}{2\zeta\omega_0} \approx \frac{\sqrt{1-\zeta^2}}{2\zeta}. \quad (35)$$

To formulate  $Q_{l2}$ , from (29), the amplitude of the damped oscillation decays exponentially with time constant  $\tau = \frac{1}{\zeta\omega_0}$ .

Therefore, after one cycle  $T = \frac{2\pi}{\omega_0\sqrt{1-\zeta^2}}$ s, the amplitude decays to  $e^{-T/\tau}$  of its original value, corresponding to an energy decay to  $e^{-2T/\tau}$ .

$$Q_{l2} = \frac{1}{1 - e^{-2T/\tau}} = \frac{1}{1 - e^{-\frac{4\pi\zeta}{\sqrt{1-\zeta^2}}}}. \quad (36)$$

When the system is under-damped,  $\zeta$  is small,

$$1 - e^{-\frac{4\pi\zeta}{\sqrt{1-\zeta^2}}} \approx \frac{4\pi\zeta}{\sqrt{1-\zeta^2}}. \quad (37)$$

Therefore,

$$Q_{l2} \approx \frac{\sqrt{1-\zeta^2}}{4\pi\zeta} = \frac{1}{2\pi} Q_{l1}. \quad (38)$$

The two definitions for the  $Q$  factor of second-order linear systems are indeed equivalent, with only a constant factor between them. This conclusion is not new, but the discussion here is useful in understanding the confusion behind the definitions of  $Q$  for nonlinear oscillators. It is arguably because of this elegant equivalence of  $Q$  definitions for second-order linear systems that we would naturally but erroneously expect that there exists a single  $Q$  definition for nonlinear systems as well, leading to some of the misconceptions and misuse of  $Q$  factors for oscillators.

In fact, as has been shown recently [16], even for linear systems, once they are not required to consist of all passive elements, the approximate equivalence in (38) can be violated — energy dissipation and bandwidth can indeed be decoupled. When it comes to nonlinear oscillators, there is no reason for us to expect a single  $Q$  that captures all the oscillator's properties; the different available definitions warrant discussions.

For oscillators, neither  $Q_{l1}$  nor  $Q_{l2}$  applies directly. Instead,  $Q$  factor is defined vaguely following the intuitions behind them. It can be done in several ways.

As mentioned in Sec. I, one definition is frequency based, using the 3dB bandwidth of the spectrum of the output of the oscillator.

$$Q_{n1} \stackrel{\text{def}}{=} \frac{f}{\Delta f_{3dB}}. \quad (39)$$

While the spectrum of the oscillating output signal indeed looks like a Bode plot, it is fundamentally different. Bode plot portrays the transfer function from the input to the output of a stable system; it is intrinsic to the system and can be calculated from system equations. For an oscillator, the sharpness of the peak observed in a spectrum analyzer depends on the noise sources present in the system. And it changes with temperature and noise level. So while  $Q_{n1}$  characterizes the frequency stability of the oscillator, it is a different quantity from  $Q_{l1}$  for linear systems.

The energy-based definition of  $Q$  factor, *i.e.*,  $Q_{l2}$ , can be extended for oscillators in more than one ways. The commonly-used definition requires calculating the total energy stored in the oscillator and the energy that is dissipated per cycle:

$$Q_{n2} \stackrel{\text{def}}{=} \frac{\text{Energy Stored}}{\text{Energy Dissipated per Cycle}}. \quad (40)$$

This definition is useful for analyzing the energy efficiency of the oscillator. But it is only meaningful when there are energy storage devices inside the oscillator. For oscillators that don't contain LC tanks, especially those outside the electrical domain, such as chemical reaction and spin-torque oscillators, it is difficult to define this  $Q_{n2}$  rigorously.

Although  $Q_{n2}$  is widely used, it represents only one way of interpreting the energy-based  $Q_{l2}$  in the context of nonlinear oscillators. In this paper, we have proposed a new definition of  $Q$ , namely  $Q_{n3}$ , that is based on perturbation on the limit cycle.

$$Q_{n3} \stackrel{\text{def}}{=} \frac{\text{Extra Energy Applied}}{\text{Extra Energy Dissipated per Cycle}}. \quad (41)$$

From our discussion in Sec. III, we can argue that this  $Q_{n3}$  is more closely analogous to  $Q_{l2}$ , as the extra amplitude and energy indeed decay to the limit cycle exponentially. The  $Q_{l2}$  for linear systems becomes a special case of  $Q_{n3}$  where the "limit cycle" is the zero state.  $Q_{n3}$  can be more rigorously formulated using the Lyapunov exponents of the system, which are analogous to the exponent for the decay of magnitude in second-order linear systems in (29). It is a quantity intrinsic to the oscillator, and can be calculated analytically or numerically from system equations.

The three  $Q$  definitions —  $Q_{n1}$ ,  $Q_{n2}$  and  $Q_{n3}$  — characterize an oscillator's frequency stability, energy efficiency, amplitude stability respectively. However, unlike in the linear resonator case, there is no direct equivalence between them. In fact, for some oscillators, they can be distinctly different. For example, a ring oscillator dissipates almost all the stored energy during each cycle; its amplitude also restores very quickly. Therefore, it has low  $Q_{n2}$  and  $Q_{n3}$ . But it can still have a large  $Q_{n1}$  based on the frequency-domain definition. Yet we rarely see reports of high- $Q$  ring oscillators, because the use of  $Q_{n2}$  is often assumed. Similar to ring oscillators, spin-torque oscillators require a DC current to sustain oscillation; they keep draining energy from the DC supply while retaining little energy in the oscillation. This means  $Q_{n2}$  should be close to 0. But high- $Q$  spin-torque oscillators have been reported with  $Q$  factors over 3000 [17]; they are analyzed based on the definition of  $Q_{n1}$  instead. This inconsistent use of terminology can create confusions for researchers if they don't have a clear understanding of the multiple  $Q$  factor definitions available for oscillators. For LC oscillators, as we show in Sec. V, with a fixed  $Q_{n2}$ , depending on the design of the nonlinearity,  $Q_{n3}$  can vary, reflecting the stability of the limit cycle of the oscillator. In this case,  $Q_{n3}$  is arguably more useful for design.

In summary, while  $Q_{l1}$ ,  $Q_{l2}$  are equivalent,  $Q_{n1}$ ,  $Q_{n2}$  and  $Q_{n3}$  are not; these quality factors characterize three separate "qualities" of nonlinear oscillators. Among them, the  $Q_{n3}$  we discuss in this paper is a new one that can be defined rigorously, characterized mathematically, calculated numerically given oscillator equations, and it has close relationship with linear systems'  $Q$  factor. It has not been studied before.

## Conclusion

In this paper, we described our ideas on defining  $Q$  factor of a nonlinear oscillator by perturbing it and assessing its amplitude stability. We discussed the mathematical formulation and numerical calculation procedures of the proposed  $Q$  definition. Results on different oscillators have validated its usefulness in the characterization of oscillators. In our further research, we plan to study the effects of the proposed  $Q$  factor on the phase noise performances of oscillators. We also intend to extend

the proposed concept and techniques to systems that are not a single oscillator, including multi-tone systems and oscillators with ancillary non-oscillatory circuitry.

*Express*, 7(2):023003, 2014.

## References

- [1] B. Razavi. A study of phase noise in CMOS oscillators. *Solid-State Circuits, IEEE Journal of*, 31(3):331–343, 1996.
- [2] M. Randall and T. Hock. General oscillator characterization using linear open-loop S-parameters. *Microwave Theory and Techniques, IEEE Transactions on*, 49(6):1094–1100, 2001.
- [3] T. Ohira. Rigorous Q-factor formulation for one-and two-port passive linear networks from an oscillator noise spectrum viewpoint. *Circuits and Systems II: Express Briefs, IEEE Transactions on*, 52(12):846–850, 2005.
- [4] W. Deng, K. Okada, and A. Matsuzawa. Class-C VCO with amplitude feedback loop for robust start-up and enhanced oscillation swing. *Solid-State Circuits, IEEE Journal of*, 48(2):429–440, 2013.
- [5] E. Vannerson and K. Smith. Fast amplitude stabilization of an RC oscillator. *IEEE Journal of Solid-State Circuits*, 9(4):176–179, 1974.
- [6] T. Wang and J. Roychowdhury. PHLOGON: PHase-based LOGic using Oscillatory Nanosystems. In *Proc. UCNC, LNCS sublibrary: Theoretical computer science and general issues*. Springer, July 2014. DOI link.
- [7] T. Wang and J. Roychowdhury. Design Tools for Oscillator-based Computing Systems. In *Proc. IEEE DAC*, pages 188:1–188:6, 2015. DOI link.
- [8] M. Farkas. *Periodic Motions*. Springer-Verlag, New York, 1994.
- [9] A. Demir, A. Mehrotra, and J. Roychowdhury. Phase Noise in Oscillators: a Unifying Theory and Numerical Methods for Characterization. *IEEE Trans. Ckts. Syst. – I: Fund. Th. Appl.*, 47:655–674, May 2000. DOI link.
- [10] K.S. Kundert, J.K. White, and A. Sangiovanni-Vincentelli. *Steady-state methods for simulating analog and microwave circuits*. Kluwer Academic Publishers, 1990.
- [11] J.W. Bandler, R.M. Biernacki, and S.H. Chen. Harmonic balance simulation and optimization of nonlinear circuits. In *Proc. IEEE ISCAS*, volume 1, pages 85–88, May 1990.
- [12] T. Wang, K. Aadithya, B. Wu, J. Yao, and J. Roychowdhury. MAPP: The Berkeley Model and Algorithm Prototyping Platform. In *Proc. IEEE CICC*, pages 461–464, September 2015. DOI link.
- [13] MAPP: The Berkeley Model and Algorithm Prototyping Platform. Web site: <https://github.com/jaijeet/MAPP/wiki>.
- [14] J. Roychowdhury. Exact Analytical Equations for Predicting Nonlinear Phase Errors and Jitter in Ring Oscillators. In *Proc. IEEE Conf. VLSI Design*, January 2005.
- [15] K. Camsari, S. Ganguly, and S. Datta. Modular approach to spintronics. *Scientific reports*, 5.
- [16] K.L. Tsakmakidis, L. Shen, S.A. Schulz, X. Zheng, J. Upham, X. Deng, H. Altug, A.F. Vakakis, R.W. Boyd. Breaking Lorentz reciprocity to overcome the time-bandwidth limit in physics and engineering. *Science*, 356(6344):1260–1264, 2017.
- [17] H. Maehara, H. Kubota, Y. Suzuki, T. Seki, K. Nishimura, Y. Nagamine, K. Tsunekawa, A. Fukushima, H. Arai, T. Taniguchi, and others. High Q factor over 3000 due to out-of-plane precession in nano-contact spin-torque oscillator based on magnetic tunnel junctions. *Applied Physics*